# Linear Quadratic AMD Controller for Five-Story Building under Seismic Ground Motion

L. Guenfaf and S. Allaoua

LSEI Laboratory, USTHB University BP 32 El Alia 16111, Bab Ezzouar, Algiers, Algeria
(e-mail: *lakhdar.guenfaf @ yahoo.fr allaoua.sofiane@ yahoo.fr*).

***Abstract*-- This study investigated a linear quadratic AMD controller for five-story building under seismic ground motion. A critical review of classical optimal control algorithms is presented in this paper for the control of the electric-type active mass driver (AMD) system. Composed primarily of an electric servomotor and a ball screw, the electrical AMD system is free from noise problems, oil leakage, and labor-intensive maintenance that commonly are associated with hydraulic AMD systems. A numerical simulation is performed using a five-story steel frame under the Kanai-Tajimi seismic ground acceleration. The AMD system performances for different weighting factors values $(R)$ are assessed. The reductions of the peak responses can reach as high as 65% and the proposed system is recommended for practical implementation.**

***Keywords*--Active mass driver, optimal control, active control, electric actuators, earthquake.**

## I. Introduction

Control algorithms for linear systems are well developed and have been extensively studied. Optimal control algorithms are based on the minimization of a quadratic performance index whose objective is to maintain the desired system state while minimizing the control effort. The active structural control system is widely used to minimize the response of structures subjected to dynamic excitations such as strong earthquakes and high winds etc [3].

In the design of tall or slender buildings, it is not only required that structural safety in the event of extreme earthquakes be guaranteed, but also that good habitability of working or residential floors be maintained in the event of strong winds or small to moderate earthquakes. The so-called 'passive vibration-control' systems, such as various configurations of steel dampers, visco-elastic dampers, and viscous dampers, have primarily been applied to guarantee structural safety in the event of extreme earthquakes. On the other hand, active vibration-control systems have been applied to maintain good habitability. Most active-control systems applied to buildings have included some type of mass damper. In the early application of active mass damper systems, a hydraulic jack was used as an actuator and the linear quadratic (LQ) control theory was introduced to enable the design of a control algorithm for the system [4].

An AMD system normally comprises of an actuator (either hydraulic or electric type), a servo-control system, a mass block, vibration sensors and a data acquisition system. Despite the fact that hydraulic-type AMD systems have been studied extensively in the laboratory [2-4], they are not favorable from a practical point of view due to problems of noise, oil leakage, and high maintenance requirements. Moreover, the peripheral equipment such as the hydraulic pump, accumulator and pipelines require additional space. On the other hand, electric servomotors are relatively clean and easy to maintain. With the rapid and revolutionary progress in power electronics and microelectronics, the commercially available AC or DC servomotors nowadays have sufficient capacity for industrial applications.

The AMD system investigated in this study is composed primarily of an AC servomotor and a ball screw. The ball screw, connected with a coupling in series, is used as the transmission media to convert the rotational motion of the motor into translation movement [2]. As the servomotor rotates one revolution counterclockwise, the mass block is advanced one pitch of the ball screw. The pitch distance of the ball screw is therefore proportional to the AMD stroke, which in turn affects the control performance of the AMD system.

In this paper, the AMD system performances for different weighting factors values $(R)$ are assessed. An instantaneous linear quadratic control algorithm is adopted, and a numerical simulation is performed using a five-story steel frame as the object structure under the conditions of a Kanai-Tajimi power spectral density function of ground acceleration. The AMD system proves to be effective and efficient for low values of the weighting factor. The reductions of the peak responses can reach as high as 65%, and the proposed system is recommended for practical implementation.

## II. Structure Model with AMD

A structural dynamic system implemented with an active mass driver system (figure 1) and subjected to earthquake ground motion, $\ddot{x}_g(t)$ and control force, $u(t)$, can be described as [3-12-13]

$$\underline{\underline{M}}\,\underline{\ddot{x}}(t)+\underline{\underline{C}}\,\underline{\dot{x}}(t)+\underline{\underline{K}}\,\underline{x}(t)=\underline{\underline{B}}\,u(t)-\underline{\underline{E}}\,\ddot{x}_g(t) \qquad (1)$$

Where

1. $\underline{x}$ is the (6×1) displacement vector

2. $\underline{\underline{M}}$ is the (6×6) mass matrix
3. $\underline{\underline{C}}$ is the (6×6) damping matrix
4. $\underline{\underline{K}}$ is (6×6) stiffness matrix
5. $u(t)$ is the control force
6. $\underline{\underline{B}}$ is the (6×1) location matrix of the control forces
7. $\ddot{x}_g(t)$ is the earthquake ground acceleration
8. $\underline{\underline{E}}$ is the (6×1) location matrix of the earthquake ground acceleration

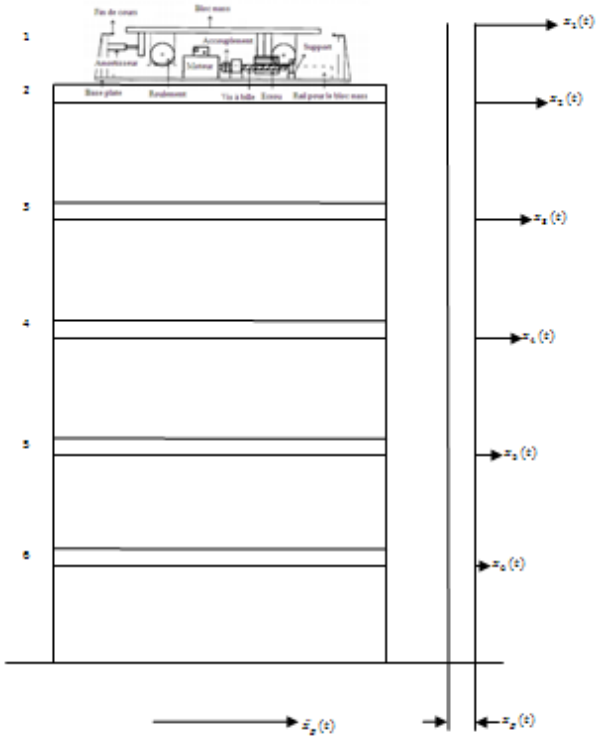

Fig. 1. A structural dynamic system implemented with an active mass driver system

The control force, $u(t)$, can be further expressed in terms of the torque, $\Gamma$, of the servomotor [2]. As the servomotor rotates one revolution, the mass block is advanced one pitch of the ball screw. Hence, the stroke of the mass block relative to the attached floor can be calculated as:

$$\bar{x}_a = x_a - x_n = \underline{L}_T x = \frac{l_b \theta_m}{2\pi} \tag{2}$$

Where $\bar{x}_a$ is the stroke of the mass block relative to the roof; $x_a$ is the displacement of the mass block relative to the ground; $x_n$ is the roof displacement of the structure relative to the ground; $\underline{L} = [1 \quad -1 \quad 0 \quad 0 \quad 0 \quad 0]^T$ is the 6×1 location vector; $\theta_m$ is the angular rotation of the servomotor; and $l_b$ is the pitch distance of the ball screw. The velocity of the mass block relative to the roof can be calculated by taking the derivatives of both sides of Equation (2) with respect to time $t$ as:

$$\dot{\bar{x}}_a = \underline{L}_T \dot{x} = \frac{l_b}{2\pi}\dot{\theta}_m = \frac{l_b}{2\pi}\omega_m \tag{3}$$

where $\dot{\bar{x}}_a$ is the velocity of the mass block relative to the roof; and $\omega_m = \dot{\theta}_m \ (rad/\sec)$ is the angular velocity of the servomotor. Similarly, the acceleration of the mass block relative to the roof can be represented as:

$$\ddot{\bar{x}}_a = \underline{L}_T \ddot{x} = \frac{l_b}{2\pi}\dot{\omega}_m = \frac{l_b}{2\pi}\alpha_m \tag{4}$$

where $\ddot{\bar{x}}_a$ is the acceleration of the mass block relative to the roof, and $\alpha_m = \dot{\omega}_m \ (rad/\sec^2)$ is the angular acceleration of the servomotor. Assuming conservation of energy, the work done by the servomotor in one revolution is equal to that of the mass block advancing one pitch. Therefore, the torque, $\Gamma$, supplied by the servomotor and the translation force, $u$, applied to the mass block satisfies

$$\Gamma = \frac{l_b}{2\pi}u \tag{5}$$

The reaction force of $u$ to the structure is the active control force. If the inertia of the rotating components, including the rotor of the servomotor, the ball screw and the coupling are taken into account, equilibrium of the torque is modified as:

$$\Gamma = \frac{l_b}{2\pi}u + (J_M + J_B + J_C)\alpha_m$$

$$\Gamma = \frac{l_b}{2\pi}u + \bar{J}\alpha_m \tag{6}$$

where $J_M$, $J_B$ and $J_C$ are, respectively, the mass moments of inertia of the rotor of the servomotor, the ball screw and the coupling; $\bar{J} = J_M + J_B + J_C$ is the sum of the mass moments of inertia of the rotating parts. Substituting Equation (4) into Equation (6), the torque supplied by the servomotor can be expressed as:

$$\Gamma = \frac{l_b}{2\pi}u + \frac{2\pi}{l_b}\bar{J}\underline{L}_T\ddot{x} \tag{7}$$

Moreover, the active control force applied to the structure can be calculated from Equation (7) as:

$$u = \frac{2\pi}{l_b}\Gamma - \left(\frac{2\pi}{l_b}\right)^2 J\underline{L}^T\ddot{\underline{x}} \tag{8}$$

By substituting the active control force from Equation (8) into Equation (1), the equation of motion of the dynamic system implemented with the AMD system driven by the servomotor, can be expressed as:

$$\underline{\underline{\bar{M}}}\ddot{\underline{x}}(t) + \underline{\underline{C}}\dot{\underline{x}}(t) + \underline{\underline{K}}\underline{x}(t) = \underline{\underline{\bar{B}}}\Gamma(t) - \underline{\underline{E}}\ddot{x}_g(t) \tag{9}$$

Where $\underline{\underline{\bar{M}}} = \underline{\underline{M}} + \left(\frac{2\pi}{l_b}\right)^2 J\underline{\underline{B}}\underline{L}^T$ is the (6×6) modified mass matrix, taking into account the inertia of the rotating parts of the AMD system; and $\underline{\underline{\bar{B}}} = \left(\frac{2\pi}{l_b}\right)\underline{\underline{B}}$ is the (6×1) location matrix of the control torques supplied by the servomotor.

## III. CONTROL ALGORITHM

### A. continuous-time state space system

Equation (9) can be further represented in a state-space form, leading to a first-order differential equation as:

$$\dot{\underline{z}}(t) = \underline{\underline{A}}_c \underline{z}(t) + \underline{\underline{B}}_c \underline{\Gamma}(t) - \underline{\underline{E}}_c \ddot{\underline{x}}_g(t) \tag{10}$$

Where

$\dot{\underline{z}}(t) = \begin{bmatrix} \underline{x}(t) \\ \dot{\underline{x}}(t) \end{bmatrix}$ is the $2n\times1$ state vector,

$\underline{\underline{A}}_c = \begin{bmatrix} \underline{\underline{0}} & \underline{\underline{I}} \\ -\underline{\underline{M}}^{-1}\underline{\underline{K}} & -\underline{\underline{M}}^{-1}\underline{\underline{C}} \end{bmatrix}$ is the $2n\times2n$ continuous-time system matrix, $\underline{\underline{B}}_c = \begin{bmatrix} \underline{\underline{0}} \\ -\underline{\underline{M}}^{-1}\underline{\underline{B}} \end{bmatrix}$ is the $2n\times1$ continuous-time location matrix of the control forces, $\underline{\underline{E}}_c = \begin{bmatrix} \underline{\underline{0}} \\ -\underline{\underline{M}}^{-1}\underline{\underline{E}} \end{bmatrix}$ is the $2n\times$q continuous-time location matrix of the earthquake ground acceleration, $\underline{\underline{0}}$ and $\underline{\underline{I}}$ denote the null matrix and the identity matrix of appropriate dimensions, respectively.

### B. Classical linear optimal control algorithm

Control algorithms for linear systems are well developed and have been extensively studied. Optimal control algorithms are based on the minimization of a quadratic performance index whose objective is to maintain the desired system state while minimizing the control effort [12-13]. For a linear system, this performance index can be defined as

$$J = \int_0^{t_f} \left[ \underline{z}^T(t) \underline{\underline{R}} \underline{z}(t) + \underline{\Gamma}^T(t) \underline{\underline{Q}} \underline{\Gamma}(t) \right] dt \tag{11}$$

in which $\underline{\underline{Q}}$ is a ($2n$ x $2n$) weighting matrix for the structural response that should be at least positive semi-definite, and $\underline{\underline{R}}$ is a ($r$ x $r$) weighting matrix for the control force that should be positive definite matrix. And $t_f$ is the duration of the excitation.

To minimize the performance index given by equation (11) subjected to the constraint equations of motion represented by the state equation (10), these two equations are adjointed with the multiplier function $\underline{\lambda}(t)$.

$$\tilde{J} = \int_0^{t_f} \left\{ \left[ \underline{z}^T(t) \underline{\underline{Q}} \underline{z}(t) + \underline{\Gamma}^T(t) \underline{\underline{R}} \underline{\Gamma}(t) \right] + \underline{\lambda}^T(t) \left[ \underline{\underline{A}} \underline{z}(t) + \underline{\underline{B}} \underline{\Gamma}(t) + \underline{\underline{W}} \ddot{x}_0(t) - \dot{\underline{z}}(t) \right] \right\} dt \tag{12}$$

Defining the Hamiltonian as

$$H\left[ \underline{z}(t), \underline{\Gamma}(t), \underline{\lambda}(t), \ddot{x}_g(t), t \right] = \underline{z}^T(t) \underline{\underline{Q}} \underline{z}(t) + \underline{\Gamma}^T(t) \underline{\underline{R}} \underline{\Gamma}(t) + \underline{\lambda}^T(t) \left[ \underline{\underline{A}} \underline{z}(t) + \underline{\underline{B}} \underline{\Gamma}(t) + \underline{\underline{W}} \ddot{x}_g(t) \right] \tag{13}$$

where $\underline{\lambda}(t)$ is a $2n$-dimensional vector representing the costate variables. Integrating by parts the last term of the right side of Equation (12), we obtain

$$\tilde{J} = \int_0^{t_f} \left\{ \left[ \underline{z}^T(t) \underline{\underline{Q}} \underline{z}(t) + \underline{\Gamma}^T(t) \underline{\underline{R}} \underline{u}(t) \right] + \underline{\lambda}^T(t) \left[ \underline{\underline{A}} \underline{z}(t) + \underline{\underline{B}} \underline{\Gamma}(t) + \underline{\underline{W}} \ddot{x}_g(t) \right] \right\} dt + \int_0^{t_f} \underline{\lambda}^T(t) \dot{\underline{z}}(t) dt - \underline{\lambda}^T(t) \underline{z}(t) \Big|_0^{t_f} \tag{14}$$

and substituting equation (13) into Equation (14), one obtain

$$\tilde{J} = \int_0^{t_f} \left\{ H\left[ \underline{z}(t), \underline{\Gamma}(t), \underline{\lambda}(t), \ddot{x}_g(t), t \right] + \dot{\underline{\lambda}}^T(t) \underline{z}(t) \right\} dt - \underline{\lambda}^T(t_f) \underline{z}(t_f) + \underline{\lambda}^T(0) \underline{z}(0) \tag{15}$$

Taking the variation of $\tilde{J}$ yields

$$\delta\tilde{J} = -\underline{\lambda}^T(t_f) \delta\underline{z}(t_f) + \underline{\lambda}^T(0) \delta\underline{z}(0) + \int_0^{t_f} \left\{ \left[ \dot{\underline{\lambda}}^T(t) + \frac{\partial H}{\partial \underline{z}(t)} \right] \delta\underline{z}(t) + \frac{\partial H}{\partial \underline{\Gamma}(t)} \delta\underline{\Gamma}(t) \right\} dt \tag{16}$$

The initial condition $\underline{z}(0)=\underline{0}$ is a given constant state vector and hence $\delta\underline{z}(0)=\underline{0}$ and $\underline{z}(t_f)=\underline{0}$, then $\delta\underline{z}(t_f)=\underline{0}$. Since Equation (16) should be zero for any arbitrary variations $\delta\underline{z}$ and $\delta\underline{\Gamma}$, i.e., $\delta\tilde{J}=0$, one has

$$\frac{\partial H}{\partial \underline{\Gamma}} = 0, \quad 0 \le t \le t_f \tag{17}$$

$$\dot{\underline{\lambda}}^T = -\frac{\partial H}{\partial \underline{z}} \tag{18}$$

with the boundary conditions $\underline{\lambda}(t_f) = \underline{0}$; substituting Equation (13) into equations (17) and (18) results in the necessary conditions for the optimal solutions

$$\dot{\underline{\lambda}}(t) = -2\underline{\underline{Q}} \underline{z}(t) - \underline{\underline{A}}^T \underline{\lambda}(t) \tag{19}$$

$$\underline{\Gamma}(t) = -\tfrac{1}{2} \underline{\underline{R}}^{-1} \underline{\underline{B}}^T \underline{\lambda}(t) \tag{20}$$

the system of equation given by equations (10), (19) and (20) provide the optimal solutions for the control vector, $\underline{\Gamma}(t)$, the response state vector $\underline{z}(t)$ and the costate vector $\underline{\lambda}(t)$.

For the general case in which the control vector is regulated by the response state vector and the external excitation, we can prove that costate vector take the form

$$\underline{\lambda}(t) = \underline{\underline{P}}(t) \underline{z}(t) + \underline{q}(t); \quad \underline{\lambda}(t_f) = \underline{0} \tag{21}$$

where the first term on the right hand side indicates the closed-loop control and the second term represents the open-loop control. Matrix $\underline{\underline{P}}(t)$ and vector $\underline{q}(t)$ are determined by substituting equation (21) into equations (10), (19) and (20) leading to the following expression

$$\left[ \dot{\underline{\underline{P}}}(t) + \underline{\underline{P}}(t) \underline{\underline{A}} - \tfrac{1}{2} \underline{\underline{P}}(t) \underline{\underline{B}} \underline{\underline{R}}^{-1} \underline{\underline{B}}^T \underline{\underline{P}}(t) + \underline{\underline{A}}^T \underline{\underline{P}}(t) + 2\underline{\underline{Q}} \right] \underline{z}(t) + \dot{\underline{q}}(t) - \left[ \tfrac{1}{2} \underline{\underline{P}}(t) \underline{\underline{B}} \underline{\underline{R}}^{-1} \underline{\underline{B}}^T - \underline{\underline{A}}^T \right] \underline{q}(t) + \underline{\underline{P}}(t) \underline{\underline{W}} \ddot{\underline{x}}_g(t) = \underline{\underline{0}} \tag{22}$$

For the case where the control torque vector, $\underline{\Gamma}(t)$, is regulated by both the response state vector, $\underline{z}(t)$, and base acceleration, $\ddot{x}_g(t)$. Equation (22) can be expressed as

$$\dot{\underline{\underline{P}}}(t) + \underline{\underline{P}}(t) \underline{\underline{A}} - \tfrac{1}{2} \underline{\underline{P}}(t) \underline{\underline{B}} \underline{\underline{R}}^{-1} \underline{\underline{B}}^T \underline{\underline{P}}(t) + \underline{\underline{A}}^T \underline{\underline{P}}(t) + 2\underline{\underline{Q}} = \underline{\underline{0}}; \quad \underline{\underline{P}}(t_f) = \underline{\underline{0}} \tag{23}$$

$$\dot{\underline{q}}(t) - \left[ \tfrac{1}{2} \underline{\underline{P}}(t) \underline{\underline{B}} \underline{\underline{R}}^{-1} \underline{\underline{B}}^T - \underline{\underline{A}}^T \right] \underline{q}(t) + \underline{\underline{P}}(t) \underline{\underline{W}} \ddot{\underline{x}}_g(t) = \underline{0}; \quad \underline{q}(t_f) = \underline{0} \tag{24}$$

where $\underline{\underline{P(t)}}$ is the Ricatti matrix. Applications in structural engineering, have show that $\underline{\underline{P(t)}}$ is typically constant (i.e., each element of $\underline{\underline{P(t)}}$ remains constant) over the entire duration of earthquake excitation and drops rapidly to zero at $t_f$. In this case, the modified transient Ricatti equation (23) reduces to the steady-state matrix Ricatti equation

$$\underline{\underline{P}}\,\underline{\underline{A}} - \tfrac{1}{2}\underline{\underline{P}}\,\underline{\underline{B}}\,\underline{\underline{R}}^{-1}\underline{\underline{B}}^{T}\underline{\underline{P}} + \underline{\underline{A}}^{T}\underline{\underline{P}} + 2\underline{\underline{Q}} = \underline{\underline{0}} \tag{25}$$

and equation (24), becomes as

$$\dot{\underline{q}}(t) - \left[\tfrac{1}{2}\underline{\underline{P}}\,\underline{\underline{B}}\,\underline{\underline{R}}^{-1}\underline{\underline{B}}^{T} - \underline{\underline{A}}^{T}\right]\underline{q}(t) + \underline{\underline{P}}\,\underline{\underline{W}}\,\ddot{x}_g(t) = \underline{0} \tag{26}$$

After solving for $\underline{\underline{P}}$ (equation 25) and $\underline{q}(t)$ (equation 26) and substituting into the solution of the optimization problem posed by equation (11) with equation (10) acting as a constraint, the linear optimal control law for closed-open-loop control can be written as

$$\underline{\Gamma}(t) = -\tfrac{1}{2}\underline{\underline{R}}^{-1}\underline{\underline{B}}^{T}\underline{\underline{P}}\,\underline{z}(t) - \tfrac{1}{2}\underline{\underline{R}}^{-1}\underline{\underline{B}}^{T}\underline{q}(t) \tag{27}$$

For closed-loop control where the control vector is governed by the response state vector $\underline{z}(t)$ only, i.e., $\underline{q}(t) = 0$, Equation (26) can be reduced as

$$\underline{\Gamma}(t) = -\tfrac{1}{2}\underline{\underline{R}}^{-1}\underline{\underline{B}}^{T}\underline{\underline{P}}\,\underline{z}(t) \tag{28}$$

Figure 2, Shows an optimal closed-loop control bloc diagram.

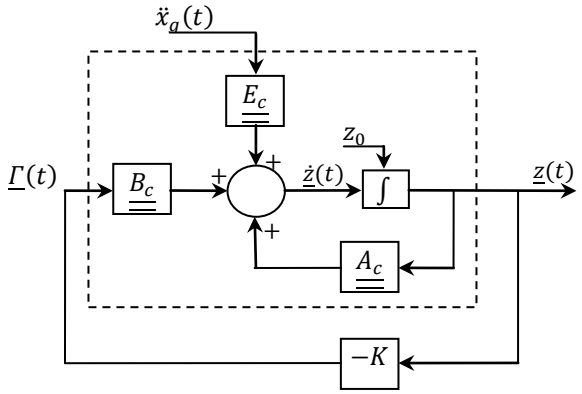


Fig 2. Optimal closed-loop control bloc diagram

Where $\underline{\Gamma}(t) = -K\underline{z}(t)$

with $K = \dfrac{1}{2}R^{-1}\underline{\underline{B}}_{C}^{T}\underline{\underline{P}}$

We are interested by regulation problem only. The tracking is not considered in this work and we have cxhoosen the infite time horizon.

## IV. Clough-Penzien Spectral Model of Earthquake Ground Motions

Modeling of earthquake strong ground acceleration, $\ddot{x}_g(t)$, as uniformly modulated non-stationary stochastic process,

$$\ddot{x}_g(t) = \psi(t)\ddot{x}(t) \tag{29}$$

Where, $\psi(t)$ is a deterministic non-negative envelope function and $\ddot{x}(t)$ is a stationary stochastic process with zero mean and a Kanai-Tajimi power spectral density function of ground acceleration

$$\Phi_g(f) = \left[\frac{1+4\xi_g^2\left(\frac{f}{f_g}\right)^2}{\left[1-\left(\frac{f}{f_g}\right)^2\right]^2 + 4\xi_g^2\left(\frac{f}{f_g}\right)^2}\right] S_0 \tag{30}$$

Where $S_0$ is the constant spectral density of the input white noise process and $f_g$, $\xi_g$ are filter parameters. However, it can be shown that the velocity and displacement spectra, which are derived from the acceleration spectra that described by equation (13), have strong singularities at zero frequencies. These singularities can be removed by using a high-pass filter, as suggested by Clough and Penzien [12]. Using such a second order high-pass filter, the Kanai-Tajimi spectrum is modified as follows:

$$\Phi_g(f) = \left[\frac{1+4\xi_g^2\left(\frac{f}{f_g}\right)^2}{\left[1-\left(\frac{f}{f_g}\right)^2\right]^2 + 4\xi_g^2\left(\frac{f}{f_g}\right)^2}\right]\left[\frac{\left(\frac{f}{f_c}\right)^2}{\left[1-\left(\frac{f}{f_c}\right)^2\right]^2 + 4\xi_c^2\left(\frac{f}{f_c}\right)^2}\right] S_0 \tag{31}$$

Various types of envelope function $\psi(t)$ have been used in the literature. A particular envelope function given in the following will be used

$$\psi(t) = \begin{cases} 0 & t < 0 \\ \left(\dfrac{t}{t_1}\right)^2 & 0 \le t < t_1 \\ 1 & t_1 \le t < t_2 \\ e^{-c(t-t_2)} & t > t_2 \end{cases} \tag{32}$$

where $t_1$, $t_2$ et $c$ are parameters which should be selected appropriately to reflect the shape and duration of the earthquake ground acceleration.

## V. Numerical Simulation

The objective structure considered for assessment of the AMD system is a half-scaled 5-story steel frame model. System parameters of the model structure are presented in [2].

Considering that the electrical AMD system is placed on the roof of the model structure for seismic response control, the parameters in system equation (9) can further be expressed as:

$X = \begin{bmatrix} x_a \\ X_S \end{bmatrix}$ is the (6×1) displacement vector, where $x_a$ is the displacement of the mass block (relative to the ground), and $X_S$ is the displacement vector of the structure (relative to the ground);

$\overline{\underline{\underline{M}}} = \begin{bmatrix} m_a & \underline{0} \\ \underline{0} & \underline{\underline{M}}_s \end{bmatrix} + \left(\frac{2\pi}{l_b}\right)^2 J \underline{\underline{B}} \underline{L}^T$ is the (6×6) mass matrix, where $\underline{\underline{M}}_s$ is the mass matrix of the structure, and $m_a = 400kg$ is the mass of the mass block, which is about 10% of the structure's total mass; $J = 0.0018kg.S^2.m$ is the rotational inertia of the servomotor system; $\underline{L} = -\underline{\underline{B}} = [1 \quad -1 \quad 0 \quad 0 \quad 0 \quad 0]^T$;

$\underline{\underline{C}} = \begin{bmatrix} c_a & -c_a \overline{\underline{L}}^T \\ -c_a \overline{\underline{L}} & \underline{\underline{C}}_s + \overline{\underline{L}} c_a \overline{\underline{L}}^T \end{bmatrix}$ is the (6×6) damping matrix, where $\underline{\underline{C}}_s$ is the damping matrix of the structure, $c_a = 204.96kg.S/m$ is the damping coefficient of the AMD system, and $\overline{\underline{L}} = [1 \quad 0 \quad 0 \quad 0 \quad 0]^T$;

$\underline{\underline{K}} = \begin{bmatrix} k_a & -k_a \overline{\underline{L}}^T \\ -k_a \overline{\underline{L}} & \underline{\underline{K}}_s + \overline{\underline{L}} k_a \overline{\underline{L}}^T \end{bmatrix}$ is the (6×6) stiffness matrix, where $\underline{\underline{K}}_s$ is the stiffness matrix of the structure, and $k_a$ is the stiffness of the AMD system ( $k_a = 0$ in the present case) ;

$\underline{\underline{E}} = \begin{bmatrix} m_a \\ 1 m_s \end{bmatrix}$ is the (6×1) location matrix of the earthquake force with $1 = [1 \quad 1 \quad 1 \quad 1 \quad 1]^T$; and $\overline{\underline{\underline{B}}} = \left(\frac{2\pi}{l_b}\right) \underline{\underline{B}}$ is the (6×1) location matrix of the control force in terms of torque.

In this paper, the weighting matrix $Q = \begin{bmatrix} \underline{\underline{K}} & \underline{\underline{0}} \\ \underline{\underline{0}} & \underline{\underline{M}} \end{bmatrix}$ is adopted to reserve meaningful physical interpretations of the first term of equation (9), as the sum of strain energy and kinetic energy of the vibrating structure.

$R$ reduces to a scalar, since only a single AMD system is implemented.

## VI. Simulation Results

In this section, the effects of the weighting factors values $(R)$ on the performance of the system are assessed. The roof acceleration history and the roof displacement history for the case of $R = 10^{-4}$ and $R = 10^{-5}$ are illustrated, respectively, in Figures 3 and 4, where large reductions of 65% in roof acceleration and 78% in roof displacement have been achieved. The torque history for the case of $R = 10^{-4}$ and $R = 10^{-5}$ is also illustrated in figure 5, where the maximum torque supplied by servomotor increases as R decreases.

## VII. Conclusion

This study investigated a linear quadratic AMD controller for five-story building under seismic ground motion. The AMD system performances for different weighting factors values $(R)$ are assessed. Moreover, an instantaneous linear quadratic algorithm was also developed. The feasibility of the proposed system was verified through numerical simulations of a five-story model structure under the conditions of a Kanai-Tajimi power spectral density function of ground acceleration. The AMD system proves to be effective and efficient for low values of the weighting factor. The reductions of the peak responses can reach as high as 65%, and the proposed system is recommended for practical implementation.

## VIII. References


[1] Chang, C.H. and Soong, T.T., *Structural control using active tuned mass dampers*, ASCE Journal of Engineering Mechanics Division, 106, 1091, 1980.

[2] Chien-Liang Lee and Yen-Po Wang, *Seismic structural control using an electric servomotor active mass driver system,* Earthquake Engineering and Structural Dynamics. 2004.

[3] Hadid, M., Afra, H. and Guenfaf, L. '*Active Control Techniques for Building Under Seismic Ground Motion*,' 1er Colloque National de GénieParasismique, ENSAG, 4, 5 et 6 Juin 1996, Bouzeréah, Vol.1, pp. 157-163.

[4] Y. Nakamura, K. Tanaka, M. Nakayama1, and T. Fujita, *Hybrid mass dampers using two types of electric servomotors: AC servomotors and linear-induction servomotor, Earthquake Engineering and Structural Dynamics. 2001.*

[5] Yang, J.N., *Control of tall buildings under earthquake excitations*, ASCE Journal of Engineering Mechanics Division, 108, 50, 1982.

[6] André Preumont, *Vibration Control of Active Structures*, Université Libre de Bruxelles, Active Structures Laboratory, Brussels, Belgium, ©2004 Kluwer Academic Publishers.

[7] André. Preumont and K. Seto, *Active control of structure*, © 2008 John Wiley & Sons.

[8] Charles K. Erdey, *Earthquake Engineering Application to Design*, Copyright © 2007 by John Wiley & Sons, Inc.

[9] Franklin Y. Chang, Hongping Jiang, Kangyu Lou, *Smart structures innovative for systems seismic response control*, 2008 by Taylor & Francis Group, CRC Press.

[10] Robert L. Williams II and Douglas A. Lawrence, *Linear State-Space Control Systems, Copyright © 2007 John Wiley & Sons, Inc.*

[11] Hadid, M., Guenfaf, L., and Afra, H. '*Linear Optimal Control Theory Applied to Earthquake Engineering Problems*,' Actes de la 2ème Conférence Maghrébinesur l'Automatique, l'Electrotechnique et l'Electronique Industrielle, COMAEI'96, 3, 4 et 5, Dec. 1996, Tlemcen, Algiers, Vol. 1, pp. 43-47.

[12] L. GUENFAF, S. ALLAOUA, *Optimal Choice actuator for AMD linear quadratic controller*, International Conference on Electrical Engineering, Algiers, May 7-9, 2012.

[13] L. GUENFAF, *Sur l'application de l'automatique et des réseaux de neurones en dynamique des structures, thèse de doctorat en automatique, ENP, 2001.*

[14] S. ALLAOUA, *Techniques et Méthodes d'intégration des actionneurs électriques et des capteurs : Application à des structures soumises à des excitations sismiques, thèse de magister en électrotechnique, USTHB, 2011*

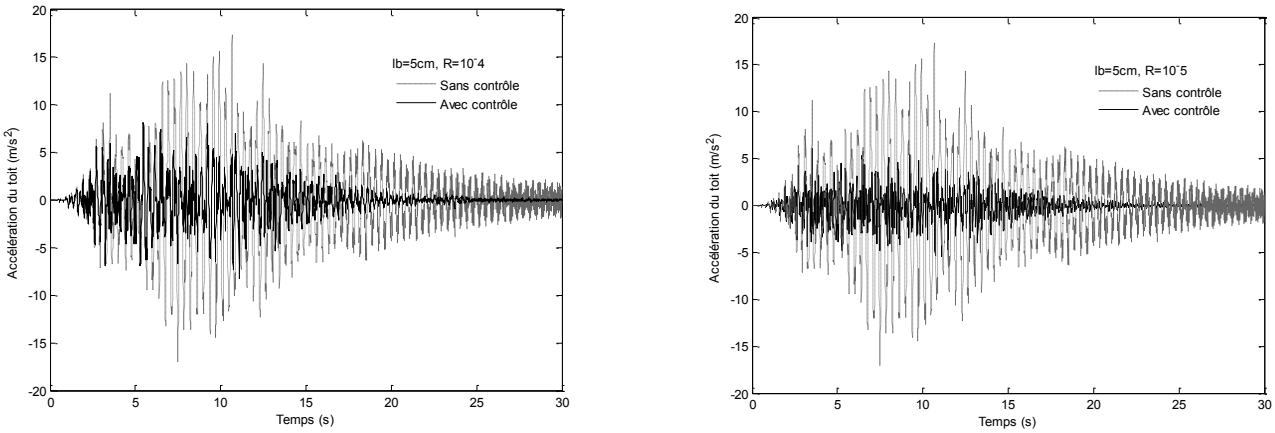


Fig. 3. Comparison of roof acceleration responses.

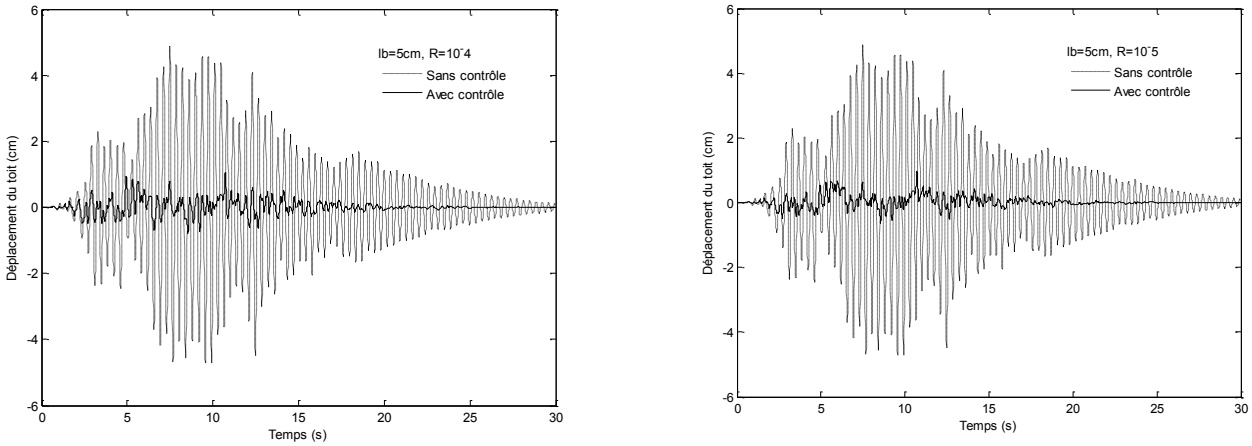


Fig. 4. Comparison of roof displacement responses.

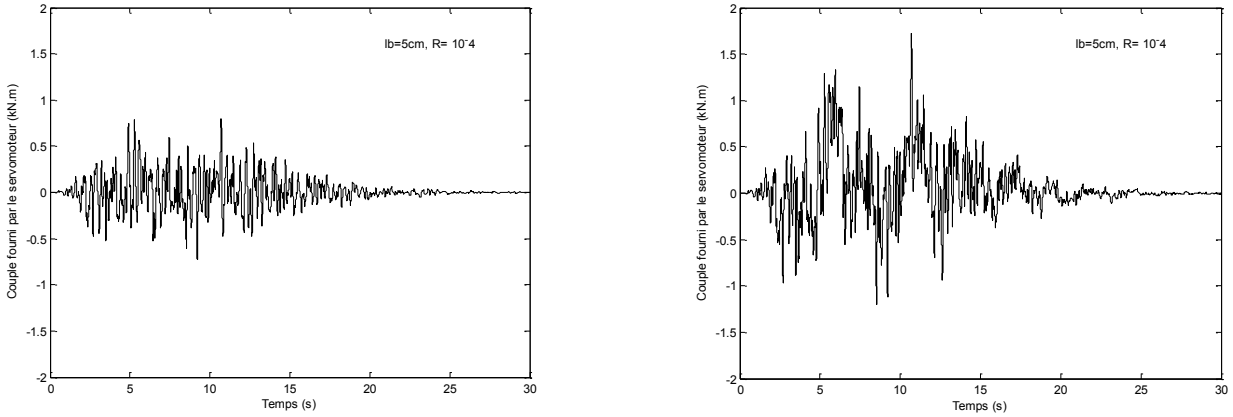


Fig. 5. Comparison torques responses